ICANS-XIII
13th Meeting of the International Collaboration on
Advanced Neutron Sources
October 11-14, 1995
Paul Scherrer Institut, 5232 Villigen PSI, Switzerland

EVALUATION OF ROTAX

H Tietze-Jaensch[1,2], W Schmidt[2,3], R Geick[4] and G Will[5]

1 ISIS Facility, Rutherford Appleton Laboratory, Chilton OX11 0QX, U.K.
2 KFA Forschungszentrum Jülich GmbH, D-52425 Jülich, Germany
3 ILL Grenoble, Centres des Tri, F-38042 Grenoble, France
4 Physikalisches Institut, Universität Würzburg, Am Hubland, D-97074 Würzburg, Germany
5 Mineralogisches Institut, Universität Bonn, Poppelsdorfer Schloß, D-53115 Bonn, Germany

ABSTRACT

After the ROTAX spectrometer has been devised and installed at ISIS it is now time to conclude on its merits and problems. We are able to show that practical scans in (Q,ω) space with a nearly arbitrary scan direction, i.e. polarisation of $\vec{q}$ vs. $\vec{Q}$ are possible and feasible with no compromises on the resolution. In addition, valuable technological and methodological knowledge has been compiled, namely in the field of digitally controled and fast acting gear-less direct drives. However, ROTAX faces difficulties from an unexpectedly weak neutron flux of its beam. We shall discuss the consequences of this outcome and briefly mention its modified new application field.

1. Introduction

The principle ideas of the rotating crystal analyser spectrometer ROTAX were presented for the first time at ICANS IX held at PSI Villigen in 1986. Since then ROTAX has been devised and installed at ISIS and we gained a lot of experience.

The method of inelastic neutron spectroscopy by using the rotating analyser principle has proved to work out feasible experimental scans through (Q,E) space, and in-hand with a much enhanced scan versality. We shall emphasize once more the benefits and improvements of the rotating analyser technique when compared with triple axis, direct geometry chopper and MAX-type inverted time-of-flight spectrometers. No compromises on the resolution with respect to the spinning analyser had to be made. As for the ESS instrumentation discussions already started, we feel that rotating analyser technique deserves a serious consideration to use it at a new intense short pulsed neutron source. We shall sketch here the proposed out-line of a very promissing ROTAX '2000.

2. Comparison with other spectrometers

2.1 general

One of the major advantages of ROTAX has always been its superior flexibility designing a time-of-flight scan in (Q,ω) space [1,2]. All neutron scattering takes place under the rules of momentum and energy conservation. The simultaneous satisfaction of both laws

$$\hbar\omega = (\hbar^2/2m)\,(k_i^2 - k_f^2)$$

and

$$\vec{Q} = \vec{k}_i - \vec{k}_f$$

is described by any point on the surface of the "scattering paraboloid" (cf. fig. 1). With a triple axis spectrometer it is, in principle, possible to view any of these scattering points which, however, needs a high-flux DC-source and all sorts of flux enhancing ancillary devices like (double)-focussing monochromators and analysers etc. for an up-to-date spectrometer. The corresponding key-word on time-of-flight machines is "multiplexing" as neighbouring tof-channels may be detected quasi-simultaneously in the course of time the neutrons take for travelling through the instrument. By using a time resolved detection electronics one will obtain tof-scans penetrating an anticipated scattering point P in (Q,ω) space on the surface of the scattering paraboloid. The specific scan direction is fixed by the instrument's geometry and set-up, only on ROTAX one may temper the scan direction [1,2,3].

On all tof-machines the time step-width may well be less than one unit of the resolution, thus encounting for a real scan profile of the envisaged point P. This is measured simultaneously instead of step-by-step in the consecutive mode of a triple axis instrument.

2.2 chopper spectrometers

Fig 1a illustrates the scattering paraboloid and the tof trajectory of a direct geometry chopper spectrometer like HET/MARI or MAPS at ISIS; these intruments operate with a fixed incident neutron energy E_i. Considering one designated point P in (Q,ω) space, a probe crystal can be aligned in such a way that one detector is viewing at a scattering angle Φ and tof-scanning through P from the bottom towards the top. Using a detector array covering a whole range of $\Phi \pm n\Delta\Phi$ will enable to measure a pixelised map of $(\Delta\Phi,\Delta t)$ digits of the whole vicinity of P. All detectors view at the same scattering paraboloid because of the fixed common incident energy E_i. Certain cuts and regrouping/rebinning out of this 2-dimensional picture enable to calculate specific scans, however, a real constant-$\vec{Q}$ scan will not be possible.

2.3 inverted spectrometers

On an inverted geometry tof-spectrometer like PRISMA at ISIS [5] or elswhere [6,7] the picture becomes much more complicated (fig 1b). n scattering arms are set to constant final energies $E_f(n)$ under certain scattering angles $\Phi_0 \pm n\Delta\Phi$, whereas the sample is bathed in a white neutron beam. Hence, every arm has got its own and inverted scattering paraboloid culminating at $-E_f(n)$. Geometric constraints to avoid clashing of adjacent detectors confine the tof-trace along a line $Q_\parallel$ parallel to k_i. The

component $Q_\perp$ is kept constant for all spectrometer arms and for all time channels, thus all paraboloids focus at a point ($Q_\perp$, $-\hbar Q^2_\perp / 2m$) in (Q,ω) space where $Q_\parallel = 0$. Every detector counts the scattered intensity along its attached tof-parabola and one will obtain a tof-profile through the point P under consideration. The adjacent detector arms may be used to coarsely map the vicinity, but no further adjustment of the scan direction can yet be made. For practical purposes of single-crystal spectroscopy $Q_\perp$ must be chosen in units modulo $2\pi/d_{hkl}$ and together with the geometric range of the instrument this means, in practice, a considerable limitation of the feasibility of an experiment on Prisma. This problem is being discussed in more detail by Dorner [8].

2.4 ROTAX in particular

This problem is overcome by the use of a non-uniformly rotating analyser crystal like on ROTAX. A rotating analyser means as much as a continuous modification of the final energy $E_f(t)$. Thus one is no-longer dealing with a discrete set of scattering paraboloids rather with a whole continuum. And, as there is only one analyser, there is no clash condition, of course, like on Prisma. This means that the Prisma-constraint $Q_\perp = \text{const}$ is no longer required. The Q-trace of the tof-scan is parameterised by the Q-value of the centre-axis of the scattering paraboloids and because it may move freely on ROTAX this may be regarded as yet another illustration of the feasibility of the various tof-scans of ROTAX. In the first place we have introduced the const-$\hbar\omega$ and the const-$\vec{Q}/|Q|$ or const-Ψ scan [1,2]. And there is a generalisation of the const-Ψ scan to the whole class of "linear-Q" scans [3]. These are scans where the Q-trace of the tof-scan forms a straight line.

Technical limitations to the performance of Rotax scans is only dictated by the time frame, i.e. incident flight path L_i, and the achievable angular acceleration that is needed to move the analyser from one point to another, i.e. the power resources of the analyser drive system. The analyser does not neccessarily have to follow an analytic curve, as the analyser drive control is working on an entirely digital basis. Further, we may emphasize that we observe the vicinity of the tof-scan, thus the vicinity of the point P under consideration too, with a very high degree of pixeling resolution. This is because we employ a linear JULIOS detector array [9] of high angular/spatial resolution. This is very essential for evaluating the 2-dimensional multiplex advantage and it is the reason why ROTAX can in principle achieve more, i.e. acquire more usefull data with only one analyser than a Prisma-type machine can do with n analyser-detector assemblies.

3. Results

3.1 inelastic scattering

Starting an experiment on ROTAX has been described in detail elsewhere [10]. A ROTAX scan is designed by an interactive software package and, of course, the experimenter is required to provide his sample parameters and experimental set-up. The experimental results are then displayed as intensities vs. a 2-dimensional pattern in detector coordinates of position and time-of-flight (x,t). Every detector pixel (x,t) is uniquely related with a corresponding pixel in (Q,ω) space. The latter can be projected onto the (x,t) plane together with the Rotax analyser scan and intensity contours of the data. Fig. 2 presents an example of longitudinal LA[110] phonons of an Al crystal as

sample. Cuts at a fixed time-of-flight or detector position channel reveal const.-k_i and const.-k_f peak profiles, respectively (fig. 3), and the FWHM time width can be used to determine the energy resolution. As an alternative the detector coordinates can be transformed into (Q_1, Q_2, $\hbar\omega$) [11] from which cuts resemble the peak profiles in Q_1, Q_2 or $\hbar\omega$ direction instantaneously. This is made possible because of the high resolution 2-dimensional data acquisition with the time-resolved Julios detector. The results yields highly "TAS-like" data. As an example we present inelastic data from a Cu crystal: fig. 4a shows the LA[110] phonon dispersion with the trace of a ROTAX const-Ψ scan in extended and reduced zone schemes. The numbers are tof-tickmarks in msec. The corresponding data and the (Q,e) projection in (x,t) coordinates is shown in fig. 4b. The enlargement shows the inelastics data around the (200) Γ-point in more detail. The approx. 25% contour of the resolution is sketched as a solid line. After transforming the data into a (Q_1=[h00], Q_2=[0k0]) projection the enlargements of fig. 4b is shown in fig. 5. A profile along [110] scan direction which is almost a const.-energy scan is shown in fig 6a with the error bars on the energy axis to denote approximately the resolution; const.-k_f profiles are shown in fig. 6b.

3.2 multiplex advantage

The multiplex potential is immediately obvious from the raw data: the number of pixels used to form the scan profiles (fig. 6b) is 21, i.e. 21 TAS-like setting would be neccessary to obtain the same picture. Not mentioned the simultaneous acquisition from higher order Brillouin zones that would add-on another factor of 3 in this particular case. The scattering intensity within the limits of a resolution unit is formed from approx. 50 pixel cells. So an average overall multiplex advantage of a factor of 50 may well be regarded as realistic. This, however, is still not sufficient to compete well with TAS machines based at typically 40 times more intense reactor sources equipped with additional flux enhancing devices like focussing monochromator etc as mentioned earlier.

3.3 enhanced efficiency: PG analyser

Nevertheless, the multiplex advantage of 50 obtained on ROTAX is a very promissing figure for the instrument itself. In fact, an additional efficiency enhancement of 3 has been achieved since we were able to install a pyrolythic graphite (PG) analyser crystal of 3.5 x 5 cm^2 (w x h) size on ROTAX at the end of 1993. The graphite is framed in a dur-aluminium clamp that is itself mounted onto the analyser motor shaft directly. The height of that analyser must not exceed much of the given size to avoid fatigue and shear-off of the Al-clamp. The electronic regulation stiffness had only been reduced to 90% of the former value used for the cylindrically shaped Ge-analyser crystal [12].

3.4 resolution

From the results achieved so far we can compile the experimentally obtained values for the energy resolution in tab. 1. The figures correspond quite well to what can be achieved on Prisma [13]. In fact, ROTAX used with a fixed, non-rotating analyser is the same as Prisma with only 1 scattering arm, and since we achieve the same resolution figures we can conclude that no resolution compromises whatsoever or any other

coarsening is observed as the result of spinning the analyser. This is made possible from the improved scan regulation electronics to work hand-in-hand with a fine tuning of the synchronisation with the ISIS sync-pulse on a μsec scale (cf. fig. 4 in [17]).

Table 1: ROTAX energy resolution:

	Ge-(220)			PG-(002)			PG-(004)		
E_i (meV)	14	50	100	13	50	100	20	75	170
$\hbar\omega$ (meV)	1.8	6.5	14	1.7	7	13	2	7	16
ΔE (meV)	0.6	3.2	10	0.6	2	8	0.5	2.6	10
$\%E_i$	4%	6%	10%	5%	4%	8%	2%	3.5%	6%

4. Technical problems and solutions

It sounds ironical, but earlier results with a temporary ROTAX set-up on the ISIS test beam were easier to achieve than with the real instrument after its commissioning had started in early 1993. An evaluation of the instrument must not miss out some comments on this fact. First of all there has been approx 3-4 times more neutron flux on test beam than on than N2a position behind Prisma. Secondly, the resolution conditions (collimation and regulation band width) on the test assembly were relaxed in order to find inelastic scattering intensities easily. So much of our time in 1993 was spent tackling bugs in the regulation software of the signal processor control. And all the other odds and bits had to be set straight. Then, it was the attempt of proper cabeling and geometric positioning of the various units that caused much of the technical difficulties we faced in the course of 1994.

4.1 fault condition

The general fault-picture was a severely diminished live-time (some 10's of minutes only) of the analyser motor's induction coils with subsequent electrical flashes and short cuts in the power unit. With a power change of up to 2 GigaWatt/sec the analyser system came to an immediate halt that could not be fused properly in the short period of time. The damaging result was that not only the servo-motor of the analyser drive was burnt to scrap but the costy power-mosfets (IGBT: insulated gate bipolar transistors) in the main amplifier unit were blown-up, too; a major electrical repair was needed every time. The regulation accuracy and running properties of the motor, while still alive, were fine and over-heating could be ruled out for the shortness of the livetime. Never before during development and thorough laboratory tests this problem had ever occurred.

4.2 technical solution

An industrial report [14] on the sensitive frequency behaviour of fast acting servo-drives running on pulse-width modulated (PWM) inverters (like our system) brought us to the correct error analysis: In fact, the length of the cable between the main amps and the motor was far too high resulting in a far too high cable capacity. Operating the system at a pwm-frequency of 10kHz ment to produce over-voltages of up to 2.5

kV between the phycically spliced cables of the 3 motor induction coils. The cable insulation was not strong enough to withstand that for long and the synchronised running mode of the motor inevitably caused hot-spots to occur persistantly at the same angular position of the coils where the motor took-up maximum power. In order to avoid this, the cable length and with it its electrical capacity had to be limited drastically back to the former length of 5-10m at the period of laboratory testing. On the other side the fibre optic communication link between the signal processor and the main inverter unit was increased to 20 m. In addition we have installed specifically made choking coils in each of the 3-phase circuits. They have an inductance of 0.5mH each in the frequency range of 0-20 kHz, a much higher value above that range and, thus, act as low-pass filters.

4.3 improvements

In fact, the temperature behaviour of the analyser motor has much improved since these modifications were introduced. The operating temperature of the ROTAX scan of fig. 6, for example, was subsequently reduced from 85°C to only 47°C only. The regulation behaviour was found to be even better, because all the high frequency rippels were filtered out. Apperently they did not contribute to any decent mechanical rotation anyway. After all, the introduction these choking coils has proved to be very vital and must not be overseen in any future design. Long term running tests on the analyser motor have been performed since May 1995 with no such problem having occurred again. Fig. 7 sketches the recent modified set-up of the ROTAX analyser hardware components.

5. Future use as a diffractometer

Despite the technical and methodological success ROTAX will predominantly be used as a conventional time-of-flight diffractometer ROTAX/Diff [15]. The main reason for this is that the neutron flux is too weak to perform successfully many interesting inelastic experiments. As a diffractometer, however, ROTAX/Diff can comply much easier with recently existing demand.

5.1 time-of-flight diffraction and data processing

The set-up and operation as a diffractometer is straight forward (fig. 8). There is no need for a time-focussing set-up of the detector geometry: This becomes evident from the tof-Bragg equation and the geometric parameters of our Julios detector (fig.9a):

$$t(x) = \frac{2\,m\,d_{hkl}}{h} \left(L_i + L_f(x) \right) \sin \Phi/2$$

with (cf. fig. 9a):

$$x - x_0 = L_{f0} \; tg \left(\Phi(x) - \Phi(x_0) \right)$$

the total time-of-flight reads:

$$t(x) = \frac{2\,m\,d_{hkl}}{h} \left(L_i + L_{f0} \right) \sin 1/2 \left[tg^{-1} (x-x_0)/L_{f0} + \Phi(x_0) \right]$$

Every powder line of const d_{hkl}-value is imaged as a curved line on the detector dis-

play (fig. 10a). Yet again we image a complete mask of the detector coordinates in (x,t) onto the (elastic) Q-space or d-space. In other words, one unique d_{hkl}-value of the powder line is attached to every single pixel in (x,t). Integration of powder diffraction lines along d-values is then obtained by rebinning a histogramm of d-value pixels (fig. 10b).

5.2 time focussing

A time focussed set-up of the Julios detector (fig.9b) would not gain anything, because the powder lines of fig. 10 would appear as horizontal lines only. It would rather worsen the (spatial) resolution because the exact position of the neutron count would be determined less accurately. Last not least, the detector is simply not long enough for a time-focussed set-up at scattering angles $\Phi > 30°$.

5.3 enhanced data acquisition

Recently, a second Julios detector unit has been installed, now capable to address a 14bit (time) by 8 bit (position) and 4 byte deep data memory array of 16 MB total size [16]. With respect to the specific application this raw data field will subsequently be reduced to handable size of some 100 kB but the data acquisition is now capable to encount for the full physical time resolution of 1 μsec for the whole time window of a neutron frame.

6.) Conclusion and sketch of ROTAX '2000

6.1 neutron scattering

The rotating analyser technique has been proved successfully by experiments. Disregarding its beam flux, ROTAX performes better than its pulsed source competitors if the experimental purpose is more to look at detailed structures in (Q,ω) space. The widely arbitrate choice of scanning through a particular point P (cf. fig. 1c), with the possibility of real transverse or longitidunal polarisation of $\vec{q}$ vs. $\vec{Q}$, is advantageous for investigating structural and magnetic excitations, in particular.

The Q and energy resolution were proved to be equal to what is achieved on other spectrometers. Setting up a scan and correctly interprete the data is achieved in a similar way and not more sophisticated than on other spectrometers. ROTAX takes best advantage of the pulsed peak-flux because of its dynamics synchronisation with the source.

The use of the rotating analyser has also proved to be a very efficient filter against spurious and off-channel background. The condition for neutrons to have the "right" energy and flight direction ($\vec{k}_f$) at the appropriate time channel t_A when the analyser allows them to be scattered is simply much harder to be met. For experimental details about this dynamic background filtering confer fig. 3 in [17].

6.2 technical

Not saying that the ROTAX-technique is yet fully matured but the major technical problems seem to be solved now and the reliability and durability in the analyser drive has been achieved, eventually. There was, admittedly, the long and painful period of

bug-fixing and fine tuning of all sorts of technical bits and pieces. The whole system is fully software-controled and runs on standardised hardware. A complete copy of the analyser drive system would now cost not more than ca. 70 thousand Deutschmarks. Indeed, ROTAX is the first instrument to use active real-time components.

6.3 present limitation

At present, the performance of ROTAX scans is limited by the following factors:

1.) the power resources of the motor is limited by its electro-magnetic force (emf) and the limit of converting electric power into mechanic power or torque. Consider that the mechanic load of mounting an analyser crystal is negligible with respect to self-momentum and mechanic inertia of the motor's rotor shaft. That means the motor basicly runs free. Replacing the existing CoSm magnets by stronger and smaller $Nd_2Fe_{14}B$ magnets would increase the magnetic energy density and enable smaller and less inert rotors giving a higher power/torque ratio. This would require R&D efford in new servor-motors.

2.) The other most critical limiting factor is, indeed, the time scale or the level of average speed on which all other dynamic actions are to be performed. Consider a reduction of the time scale by a factor of 2. That would reduce the speed by 2, the acceleration by 4 and the total electric power by 8, yet enable the perfomance of many more scans on ROTAX which are at present limited purely by technical reasons.

6.4 what to do better?

1.) How to stretch the time scale? Simply by increasing the incident flight path by the same factor. This would bring ROTAX down to a position ca. 30 m off the moderator and would, inevitably push ROTAX into the domain of colder or cold neutrons. A primary path neutron guide should be used instead of a pin-hole tube not to give away too much incident flux.

2.) The analyser would then turn at only half the average speed. Yet there is a serious possibility of introducing frames to mount at least a vertically curved analyser for secondary focussing.

3.) More than one secondary flight arm may be installed, however, we don't believe that more than 2 (max. 3) could be employed reasonably.

4.) More promissing would be to install another rotating analyser on the one existing scattering arm. It could be made moveable around one analyser's axis and would give access to two simlutaneous and closely related scans. One or two detector assemblies may be used. Fig. 11a sketches an example of 2 correlated const.-Ψ scans, fig. 11b illustrates the real space geometry of such a ROTAX '2000.

5.) The pulsed source repitition frequency should not be at 50 Hz, rather adapted to avoid frame overlap at a 30 m position and allow sufficient time to rephase the analyser for the next pulse. This repositioning time is typically 2/3 of the physical scan time, i.e. the time for the neutrons to travel accross the instrument.

6.) A neutron beam-line with full flux should be made available.

6.5 promissing future?

Why not considering such an instrument for the ESS at its 10 Hz target with a cold moderator ?

Acknowledgment

We are indebted to a great number of people who have advised and helped us to develop and install the ROTAX instrument at ISIS. They can't be named all explicitly but their contribution has been very valuable. ROTAX was initiated under the hospices of the University of Würzburg and been transferred recently to be administered and further developed by the University of Bonn. Financial support was given by the German Minister for Education and Research BMBF under contract no.s 03-ge3-wue and 03-wi3-bon. The collaboration with the ISIS Facility of the Rutherford Appleton Laboratory is gratefully acknowledged. Thanks to Peter Fabi for inspiring discussions on this manuscript.

references

[1] R Geick and H Tietze, Nucl. Inst. & Meth. A 249 (1986) 325

[2] H Tietze and R Geick, Proc. ICANS IX, PSI 1986, SIN-rep. 40926 (1987) 389

[3] W Schmidt, H Tietze-Jaensch and R Geick, Proc. ICANS XII, Abingdon 1993, RAL rep. 94-025, p. I-293

[4] R S Eccleston and R Osborn, RAL rep. 94-117
S M Bennigton and R S Eccleston, RAL rep. 94-102
T G Perring, A D Taylor, R Osborn, D Mc Paul, A T Boothroyd and G Aeppli; Proc. ICANS XII, Abingdon 1993, RAL rep. 94-025, p. I-60

[5] U Steigenberger, M Hagen, R Caciuffo, C Petrillo, F Cilloco and F Sacchetti; Nucl. Instr. & Meth. B53 (1991) 87-96

[6] E Maliszowski, V V Nite, I Sosnowska and J Sosnowska; Inel. Neutron Scattering (IAEA, Vienna 1968) vol. 2, p. 313

[7] K Tajima, Y Ishikawa, K Kanai, C G Windsor and S Tomiyoshi; Nucl. Instr. & Meth. A254 (1987) 333

[8] B Dorner, J Neutron Research 2.3 (1994) 115-127

[9] E Jansen, W Sch'fer, A Szepesvary, G Will, R Reinartz, K D M[ller, H Tietze and U Steigenberger; Physica B 180 & 181 (1992) 917-919

[10] H Tietze-Jaensch, W Schmidt, R Geick and U Steigenberger; Physica B 213 & 214 (1995) 878-880

[11] W Schmidt, H Tietze-Jaensch and R Geick; Physica B 213 & 214 (1995) 881-883

[12] A Freund and C Petrillo, internal unpublished report, ISM Frascati (1987)

[13] M Hagen and U Steigenberger, Proc. ICANS XII 1993, RAL rep. 94-025, p. I-314

[14] P Hansen and F Petersen, Danfoss Drives and Controls, Graasten, Denmark 1993

[15] W Schäfer, E Jansen, R Skowronek, G Will, W Kockelmann, W Schmidt and H Tietze-Jaensch, Nucl. Inst. & Meth A (1995), in press

[16] K D M[ller, R Reinartz, R Engels, P Reinhart, J Schelton, W Sch'fer, E Jansen and G Will, Proc. workshop "new tools f. neutron instrumentation", Les Houches 1995, J Neutron Research, submitted

[17] H Tietze-Jaensch, W Schmidt and R Geick, Proc. ICANS XII, Abingdon 1993, RAL rep. 94-025, p. I-97

figure captions:

Fig. 1: scattering paraboloids at point P in (Q,E) space for a direct geometry chopper spectrometer like MAPS and the inverted geometry spectrometers PRISMA and ROTAX. Tof-trace and the same scattering triangles for P and an imaginate Q-lattice are shown in all 3 cases.

Fig. 2: Inelastic neutron scattering with a ROTAX scan along (100) direction of Al.

Fig. 3: const-k_i and const-k_f profiles of the phonons denote in fig. 2.

Fig. 4: ROTAX inelastic scattering from copper (110) direction: (a) Rotax scan parabola in extended and reduced zone scheme, (b) plot of the data and ($Q,\hbar\omega$) lattice together with the scan trace in (x,t) detector coordinates; the insert enlarges the area around the (200) Γ point.

Fig. 5: Transform of the enlargement of fig 4b into ($Q_1=(h00),Q_2=(0k0)$) coordinates with trace of energy transfer $\hbar\omega$ and scan trace.

Fig. 6: Scan profiles of the close-up of fig. 4b: (a) along Q=(110), which is almost at constant energy transfer; (b) const. k_f profiles through either phonon peak.

Fig. 7: Hardware of the ROTAX analyser drive after the 1995 improvements.

Fig. 8: Sketch of the ROTAX / Diff time of flight diffractometer after removal of the analyser tower.

Fig. 9: (a) real space detector coordinates as used for calibration and d-value line integration of powder patterns; (b) potential alignment for time-focussing set-up: All neutron energies scattered from one powder line would arrive at the same time in all position channels. As discussed in text, this set-up is obsolete on ROTAX/Diff.

Fig. 10: Example of a Ni-powder pattern obtained on ROTAX/Diff: (a) original raw data in (x,t) detector coordinates; (b) after powder-line integration discussed in text.

Fig. 11: Correlated scans of a double-ROTAX set-up for simlutaneous scanning at 2 different scattering angles Φ_1 and Φ_2.
(a) (Q,E)-parabolas of the tof traces and scattering triangles; (b) real space shape of the instrument and sketch of detector raw data.

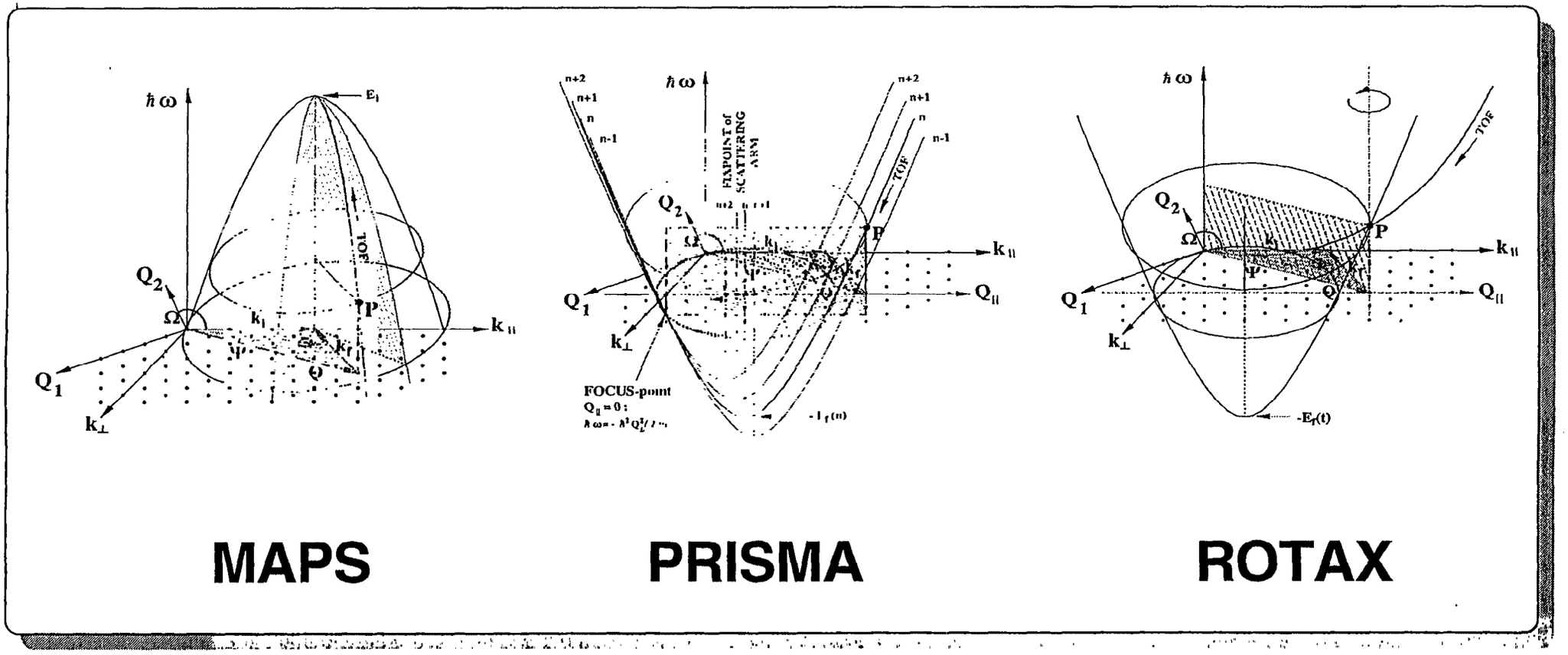

Fig. 1: scattering paraboloids at point P in (Q,E) space for a direct geometry chopper spectrometer like MAPS and the inverted geometry spectrometers PRISMA and ROTAX. Tof-trace and the same scattering triangles for P and an imaginate Q-lattice are shown in all 3 cases.

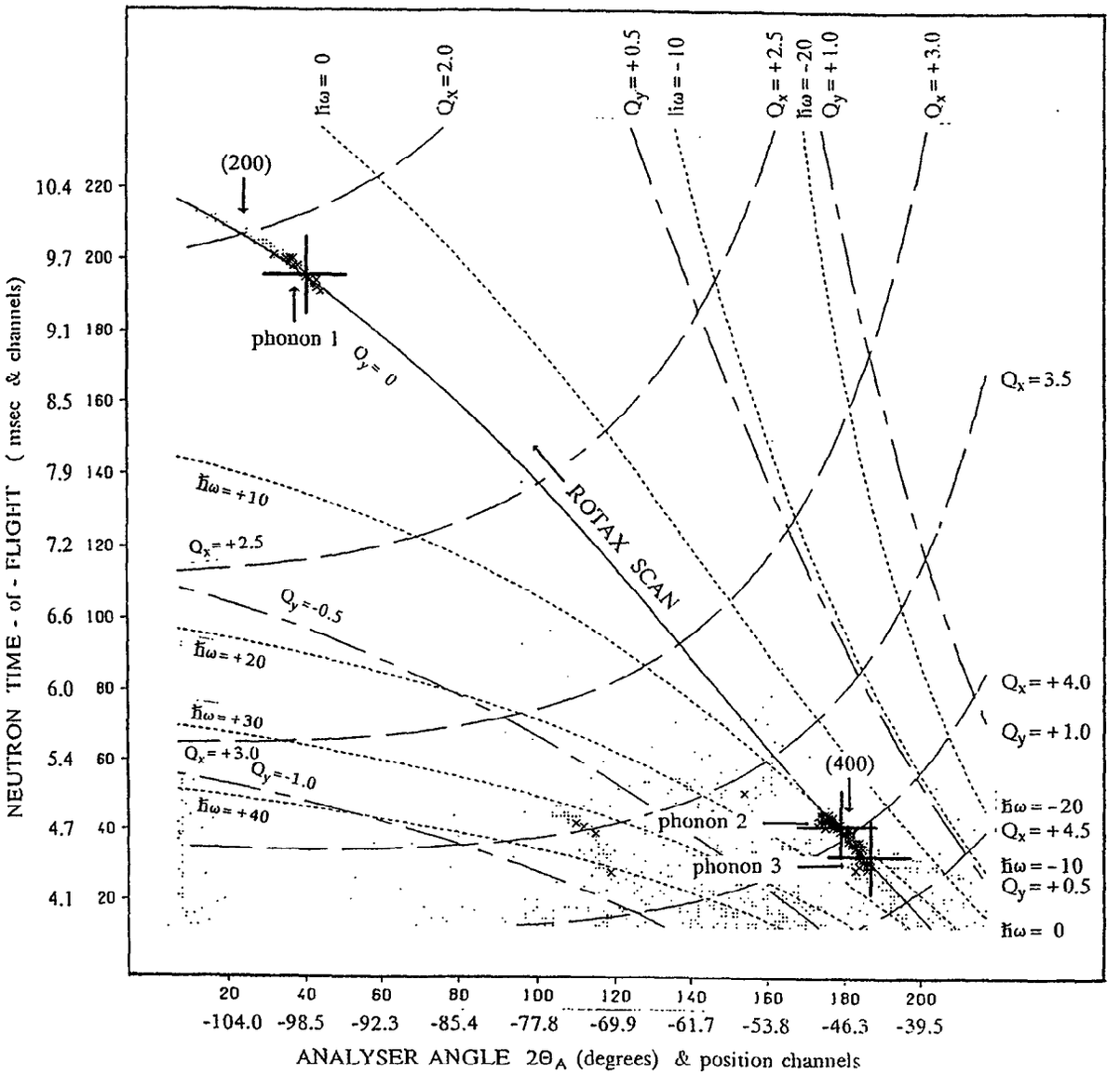

Fig. 2: Inelastic neutron scattering with a ROTAX scan along (100) direction of Al.

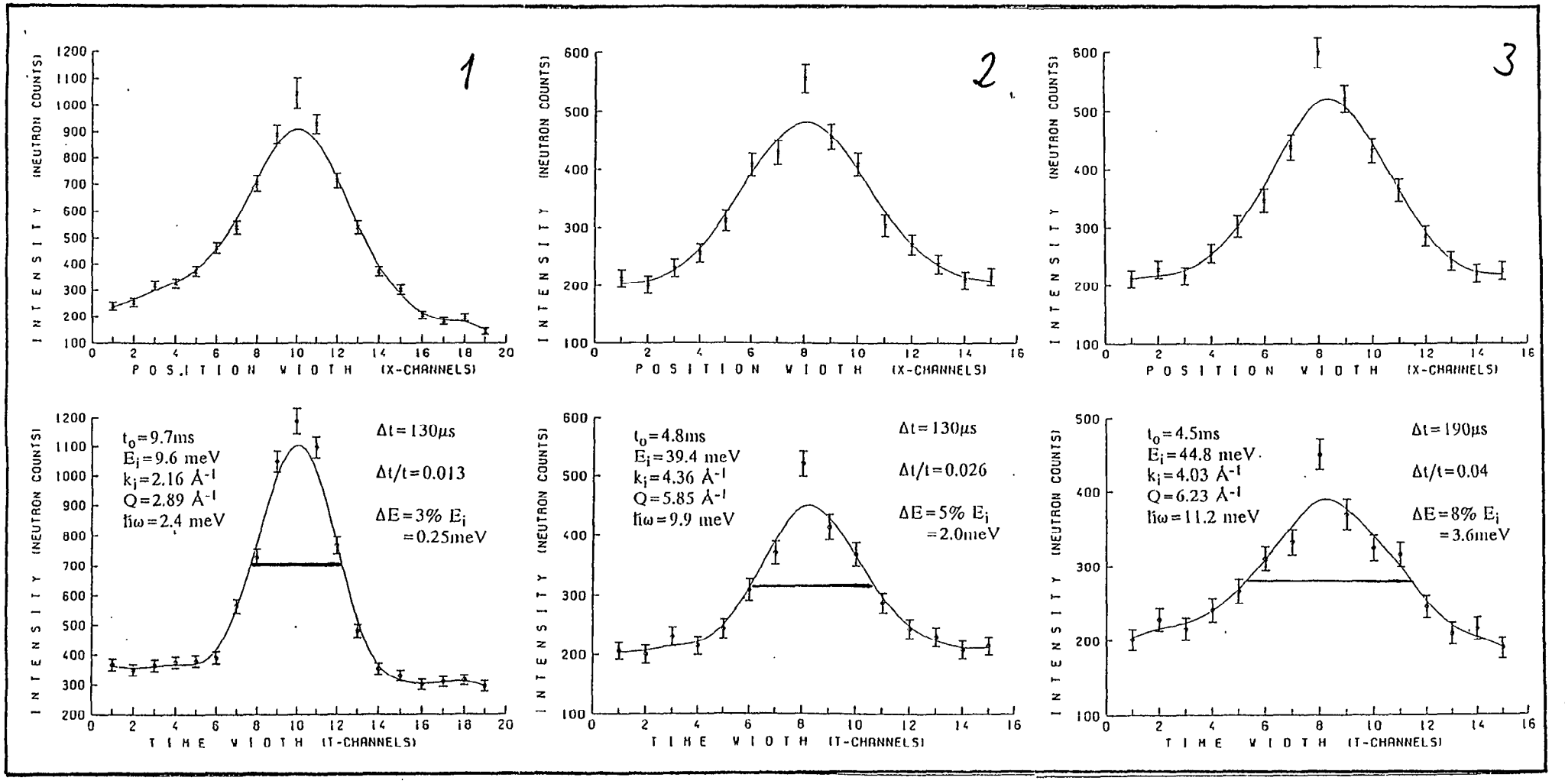

Fig.3: Intensity profiles of the phonons 1,2,3 (cf. fig.2) along position and time channels of the detector units.

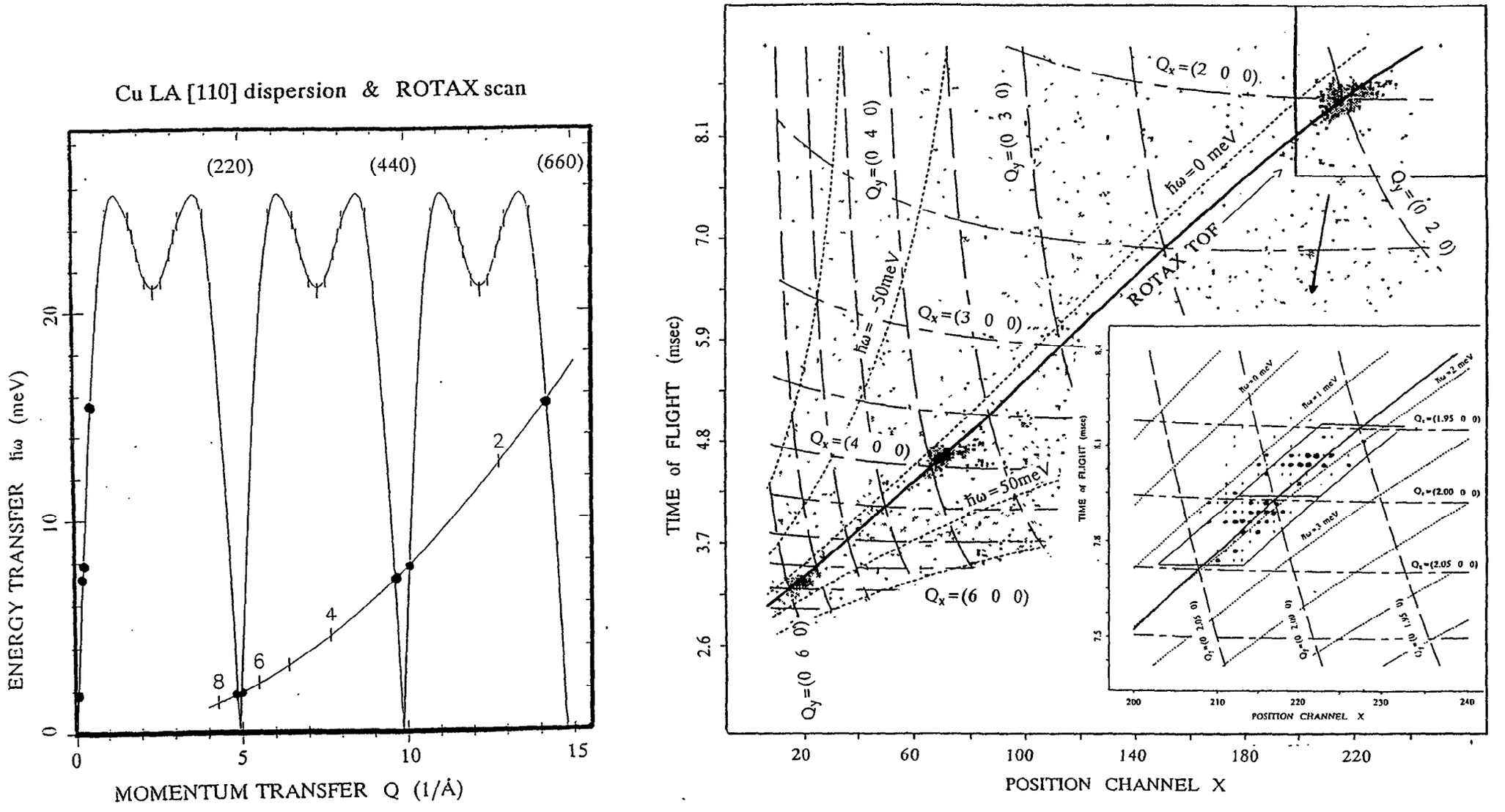

Fig. 4: ROTAX inelastic scattering from copper (110) direction: (a) Rotax scan parabola in extended and reduced zone scheme, (b) plot of the data and (Q,ħω) lattice together with the scan trace in (x,t) detector coordinates; the insert enlarges the area around the (200) Γ point.

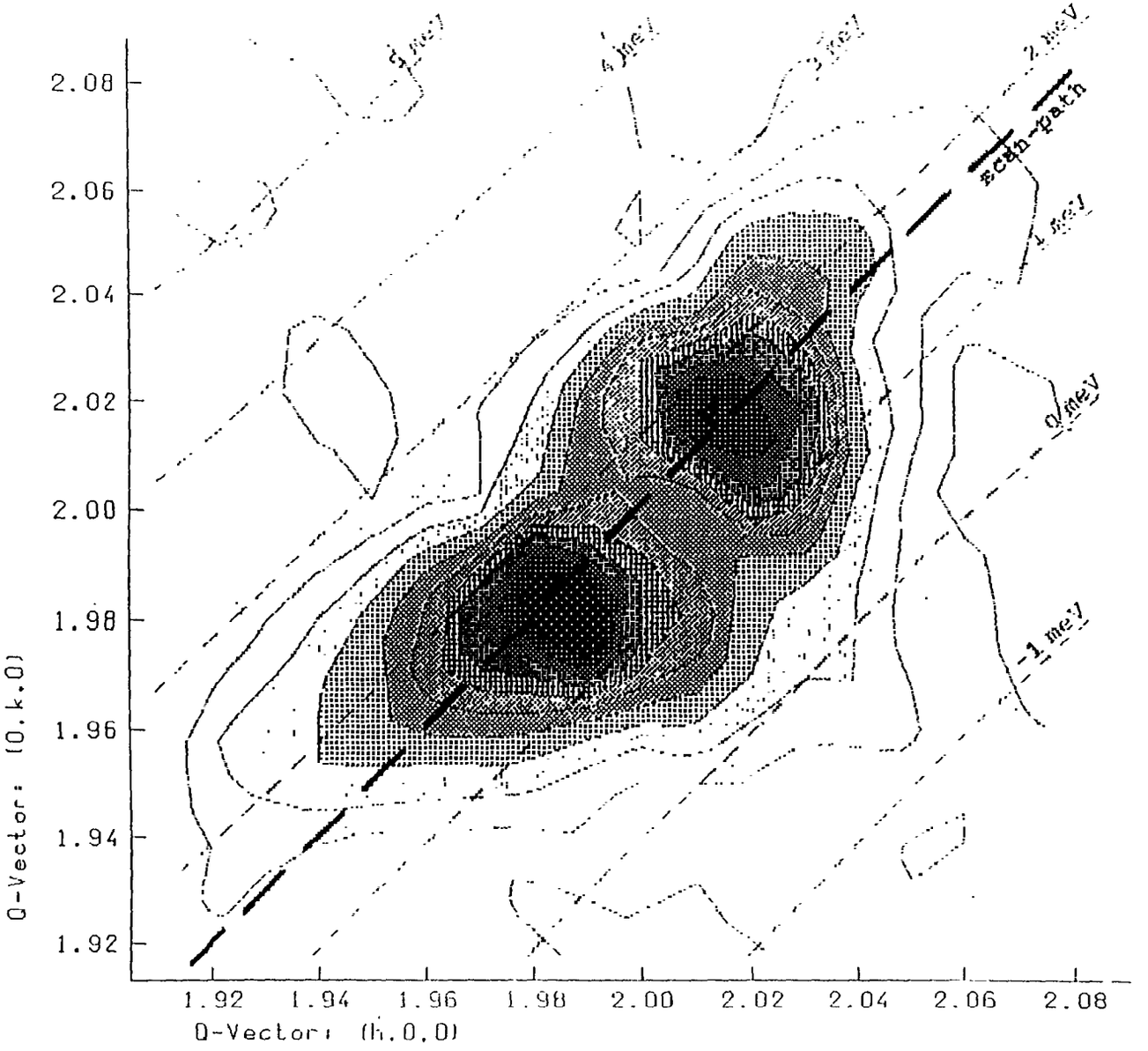

Fig. 5: Transform of the enlargement of fig 4b into (Q_1=(h00),Q_2=(0k0)) coordinates with trace of energy transfer $\hbar\omega$ and scan trace.

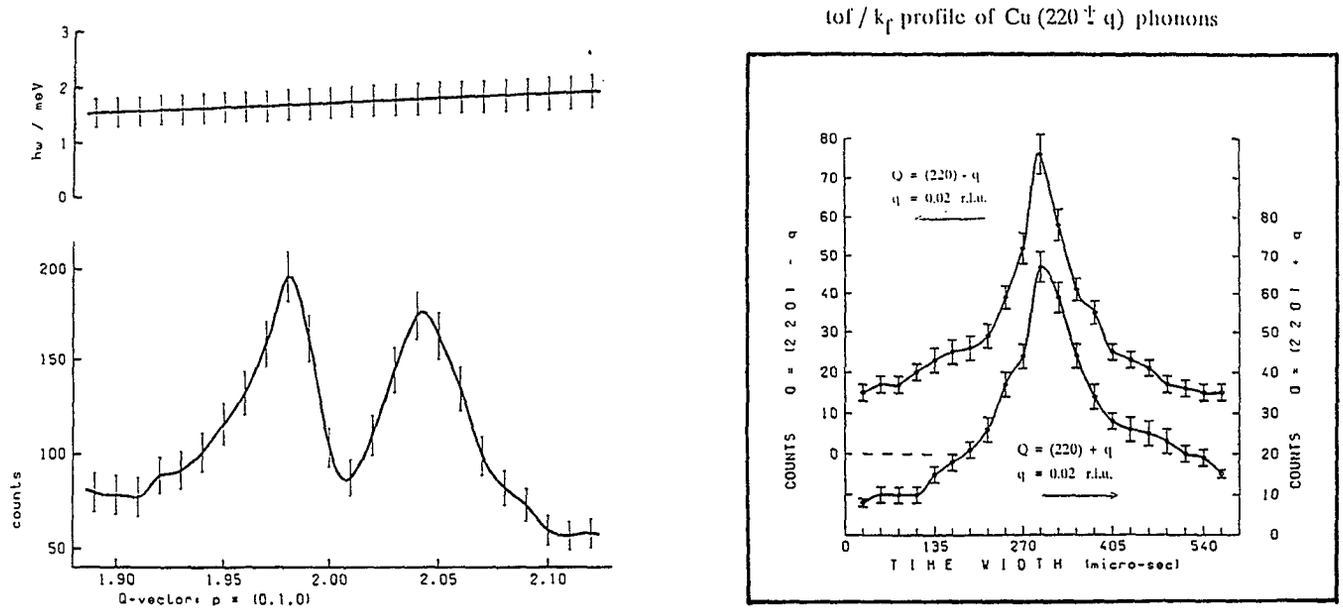

Fig. 6: Scan profiles of the close-up of fig. 4b: (a) along Q=(110), which is almost at constant energy transfer; (b) const. k_f profiles through either phonon peak.

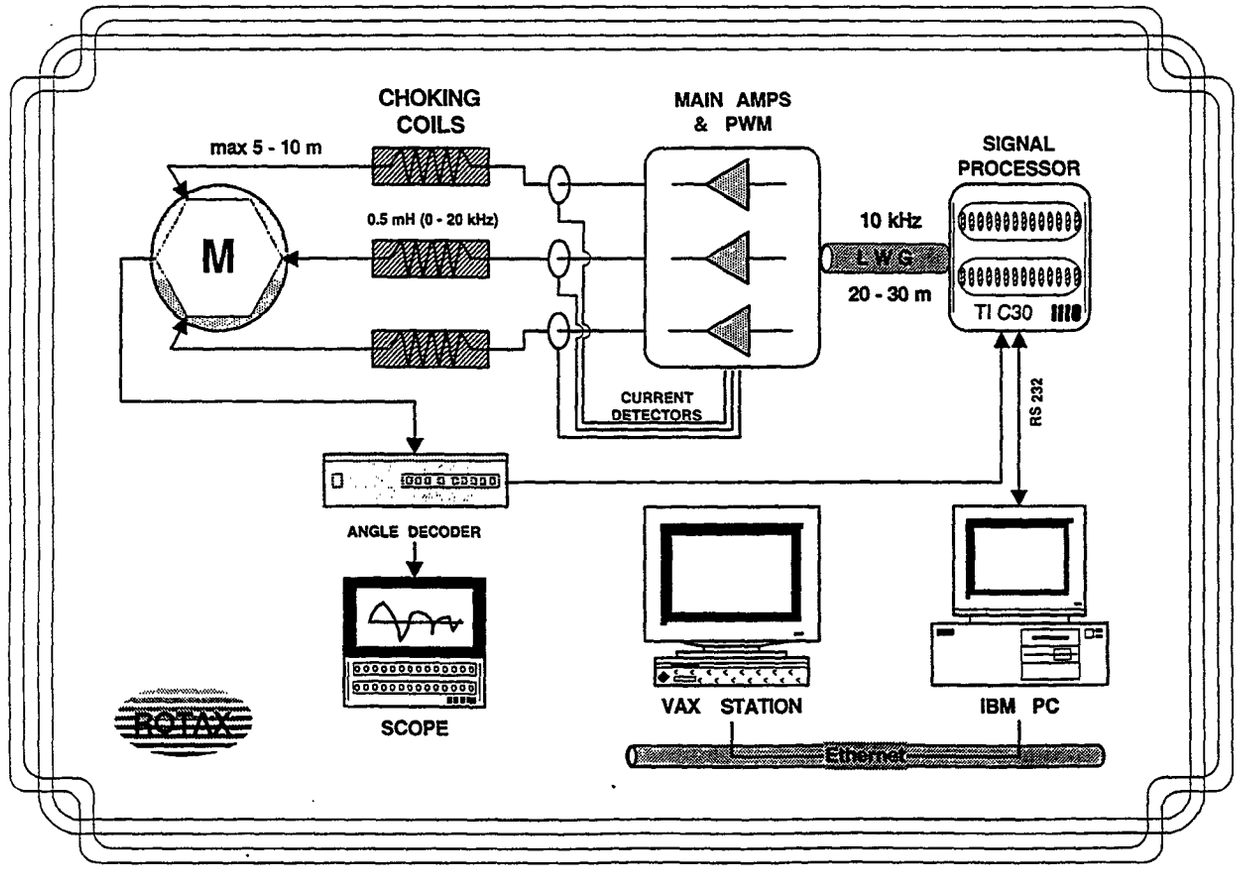

Fig. 7: Hardware of the ROTAX analyser drive after the 1995 improvements.

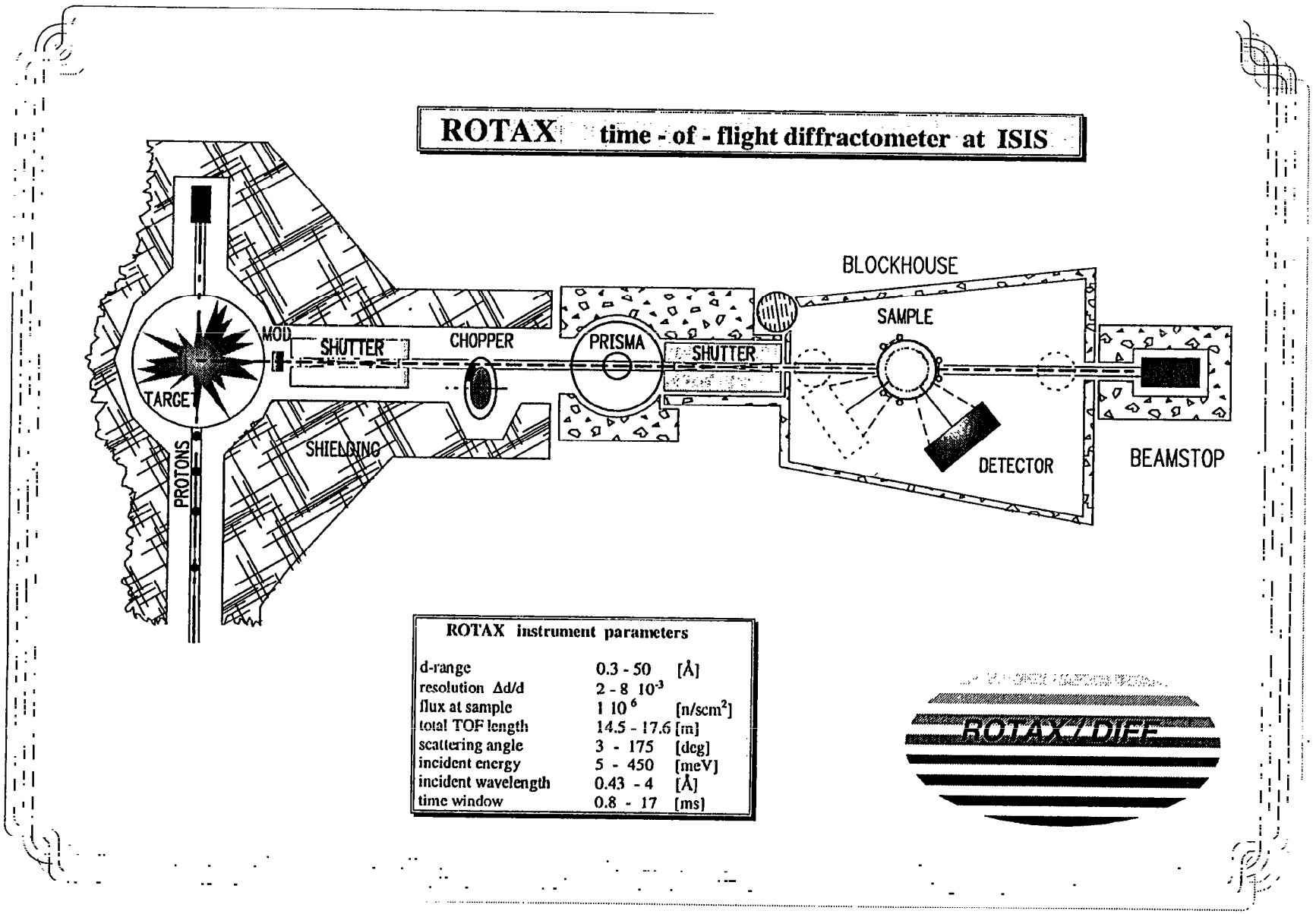

ROTAX instrument parameters

d-range	0.3 - 50	[Å]
resolution Δd/d	2 - 8 10^{-3}	
flux at sample	1 10^{6}	[n/scm^2]
total TOF length	14.5 - 17.6	[m]
scattering angle	3 - 175	[deg]
incident energy	5 - 450	[meV]
incident wavelength	0.43 - 4	[Å]
time window	0.8 - 17	[ms]

Fig. 8: Sketch of the ROTAX / Diff time of flight diffractometer after removal of the analyser tower.

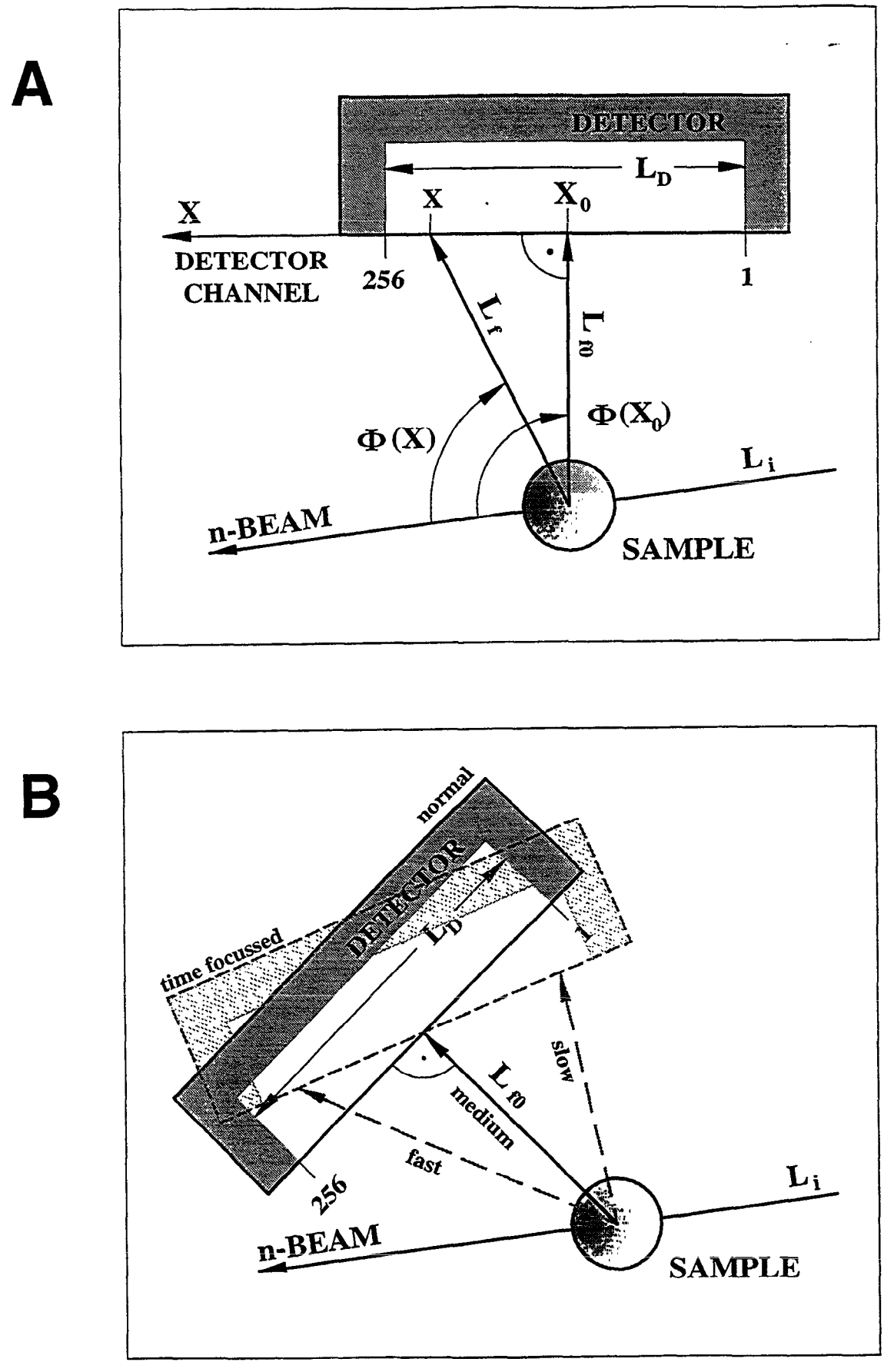

Fig. 9: (a) real space detector coordinates as used for calibration and d-value line integration of powder patterns; (b) potential alignment for time-focussing set-up: All neutron energies scattered from one powder line would arrive at the same time in all position channels. As discussed in text, this set-up is obsolete on ROTAX/Diff.

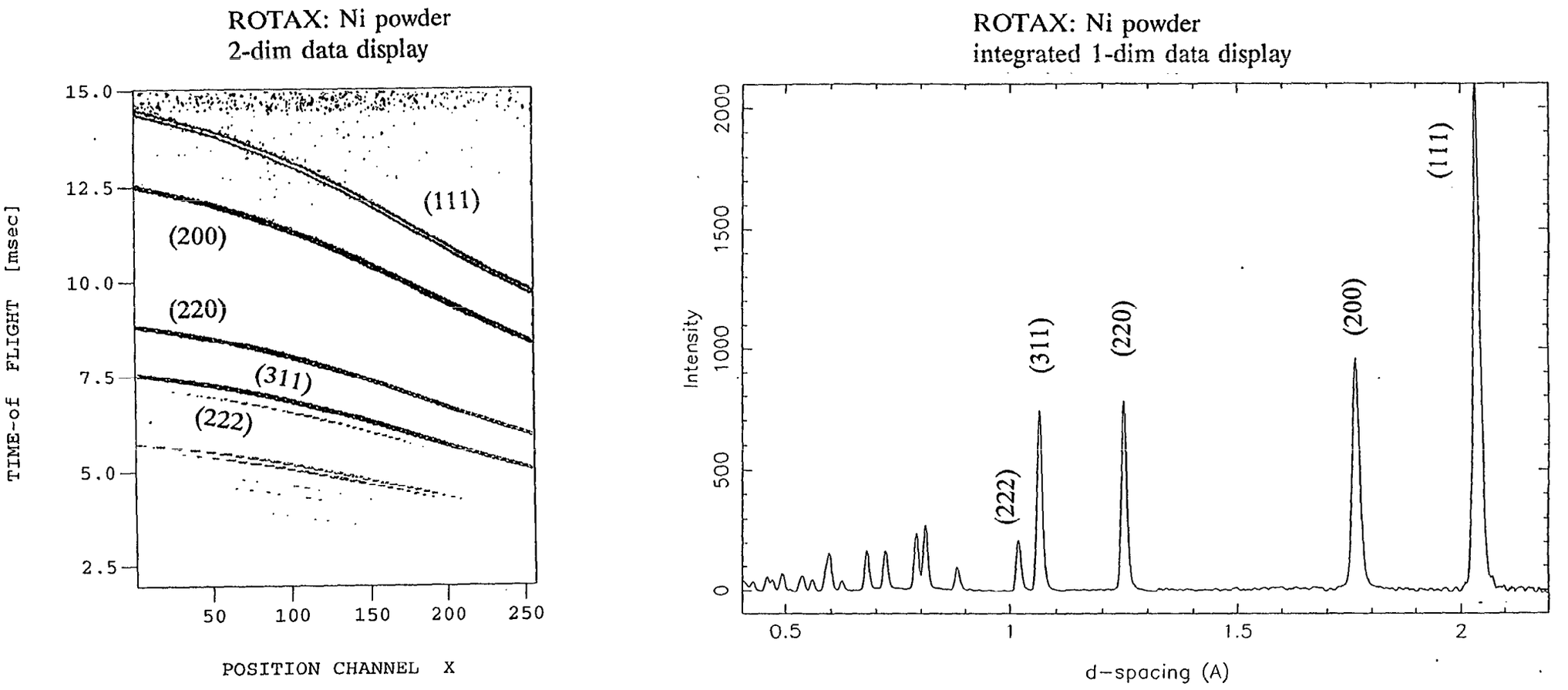

Fig. 10: Example of a Ni-powder pattern obtained on ROTAX/Diff: (a) original raw data in (x,t) detector coordinates; (b) after powder-line integration discussed in text.

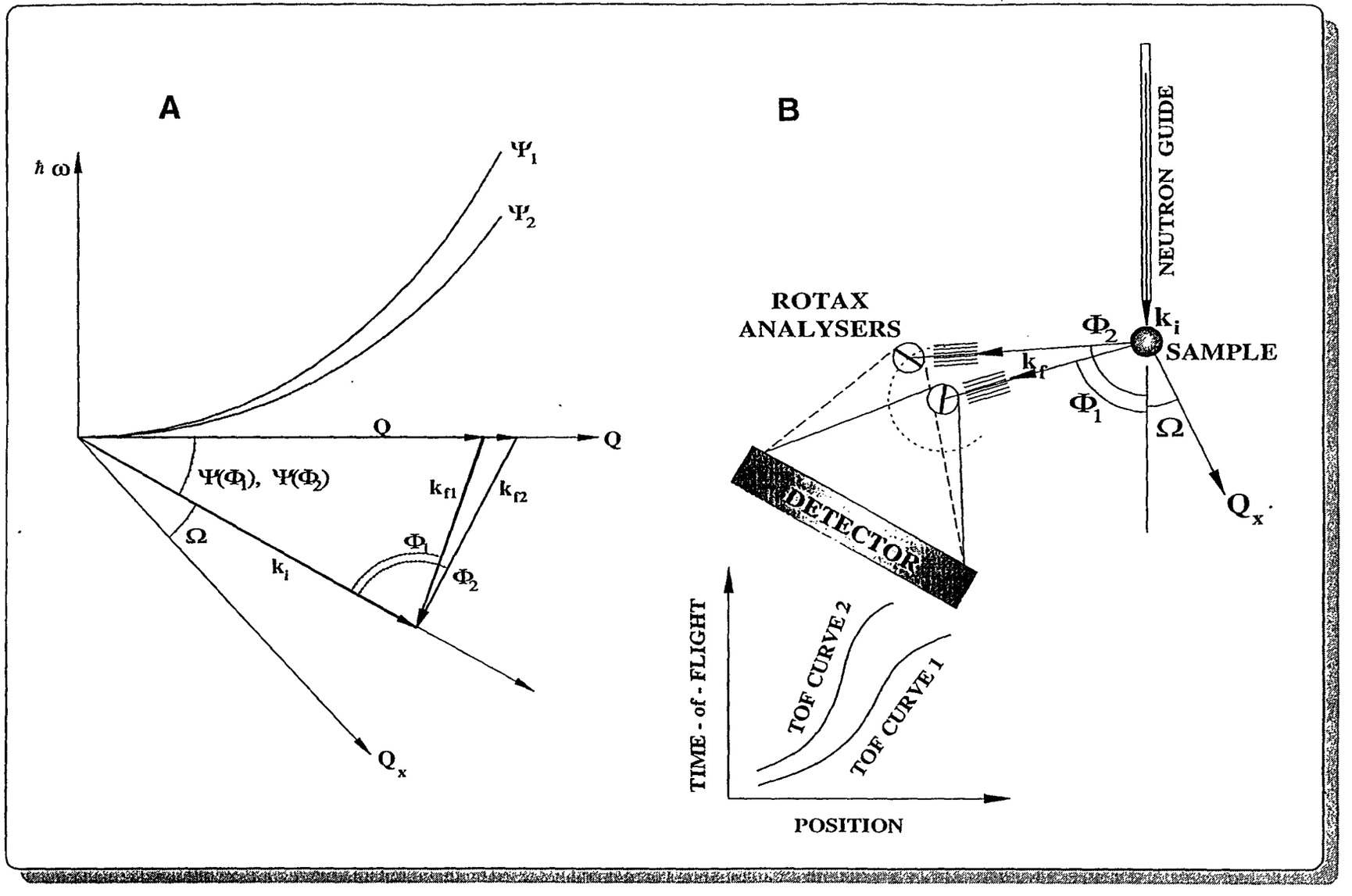

Fig. 11: Correlated scans of a double-ROTAX set-up for simlutaneous scanning at 2 different scattering angles Φ_1 and Φ_2.
(a) (Q,E)-parabolas of the tof traces and scattering triangles; (b) real space shape of the instrument and sketch of detector raw data.